Characterization of home-made graphite/PDMS microband electrodes for amperometric detection in an original reusable glass-NOA®-PDMS electrophoretic microdevice

Jérémie Gouyon, Fanny d'Orlyé, Sophie Griveau, Féthi Bedioui, Anne Varenne

Characterization of home-made graphite/PDMS microband electrodes for amperometric detection in an original reusable glass-NOA®-PDMS electrophoretic microdevice

Gouyon J.[1,2], d'Orlyé F.[1], Griveau S.[1], Bedioui F.[1], Varenne A.[1]

[1] Chimie ParisTech, PSL University, CNRS 2027, Institute of Chemistry for Life and Health Sciences, SEISAD 75005 Paris, France

[2] French Environment and Energy Management Agency, 20, avenue du Grésillé- BP 90406 49004 Angers Cedex 01 France

E-mail adress: anne.varenne@chimieparistech.psl.eu (Varenne A.)

Abstract

A new dismountable and reusable microchip for electrophoretic separation coupled to amperometric detection was developed. For this purpose, a new home made three-microbands electrode system was developed and microfabricated based on screen-printing for the inclusion of graphite/polydimethylsiloxane (C-PDMS) composite in microchannels down to 30 µm width. The composition of the composite as well as the fabrication methodology were optimized for an easy handling and an optimized electrochemical behavior. The electrochemical characterization of this composite material was first performed in bulk format (disc-shaped electrode, 6 mm diameter). It was then transposed to the micrometric scale for its integration in an original glass-NOA81®-PDMS microfluidic device allowing for reversible sealing. The microband electrodes were characterized by scanning electron microcopy and cyclic voltammetry, illustrating a good control of the microelectrode width. Then, the analytical performances of the C-PDMS composite microelectrodes were evaluated using $Ru(NH_3)_6^{3+}$ and FcMeOH as model electroactive molecules. The electrophoretic separation and quantitation of $Ru(NH_3)_6^{3+}$ were then performed in a background electrolyte made of hydrochloric acid and sodium chloride, leading to a LOD and a LOQ of 3.4 µmol.L^{-1} and 11.3 µmol.L^{-1} , respectively. The re-openable NOA-based microdevice permits to regenerate the electrode surface by simply repositioning the microband on a new spot, allowing for robust analysis in a reusable system.

Keywords

Microelectrode – Screen Printing – Chronoamperometry – Electrophoresis – Microchip

1. Introduction

Microchip electrophoresis is a separation method dedicated to short-time analysis of diluted samples when coupled with quite sensitive detection methods. Diverse strategies have been developed for detection within microfluidic channels, such as optical detections [1] (UV absorption, laser induced fluorescence (LIF)), mass spectrometry [2] or electrochemical detections [3]. The use of conductive surfaces directly integrated into the microchannels for electrochemical detection is of interest since the integration and miniaturization of electrodes are simple, allow for a good sensitivity (similar to LIF) and are relevant for the detection of many analytes, as long as they are electroactive [4].

The development of amperometric detectors in microchip electrophoresis device has been studied with different electrode materials and geometries for a wide range of applications. The main advantages of this detection mode are its low cost and easy integration into electronics since the signal is electric by nature. In addition, it provides high sensitivity in comparison to optical detection such as UV absorption. It is also possible to infer higher detection selectivity by modification of the electrode surface so as to act as a filter towards non-desirable analytes in complex matrices. Whereas the electrode surface modification may lead to the selective measurement of one target analyte, environmental and biochemical analyses often require the selective detection of several target analytes in a complex mixture. In this context, it can be relevant to integrate an upstream separation step, mainly of electrokinetic nature, in the total analysis process that would allow combining selective and sensitive measurements. Such strategy has been developed in a classical capillary format but also in microchip format [5]. In the latter format, the main challenge relies in isolating the detection system from the high separation voltage (in the order of kV) in order to preserve both signal to noise ratio and potentiostat integrity. Nowadays, commercial miniaturized devices for microchip electrophoresis with electrochemical detection are available [6], but they are still expensive due to the use of precious metals to fabricate microelectrodes, such as platinum (Pt) or gold (Au). They also do not offer the required flexibility for cleaning or reusing them easily. The use of cheaper materials for industrial production of smarter devices is therefore interesting.

Carbon-based electrodes, made from less expensive materials, have shown great interest since they allow a wide variety of atomic states and physical forms, high conductivity at low cost and generally offer a wider electrochemical potential window compared to Pt or Au. Interesting examples in the literature show the implementation of microchip electrophoresis in channels integrating carbon-based electrodes for in–line electrochemical detection (fibers [7],

inks [8], pastes [9], composites [10]) dedicated to diverse applications such as the detection of organic compounds [11]. Particularly, composites made of polydimethylsiloxane (PDMS) and carbon particles are of interest since PDMS is one of the most commonly used polymers for microfluidic applications. Carbon/PDMS (C/PDMS) was mainly used for the conception of sensors for mechanical application [12] and phosphate monitoring[13], obtained by casting appropriate C/PDMS composite in 3D-printed molds, or used as material for strain and temperature sensing[14]. Actually, the resistivity of the material changes with the temperature, allowing for good heat sensing in robotics[15] and possible piezosensor [16] since the resistivity is also affected by the composite strain. Indeed, introduced for the first time in microsystems for valves and pumps fabrication [17], C/PDMS composite conductivity and mechanical properties have been characterized [18], showing the effect of mechanical stress on the electrical capacity.

C/PDMS can also be used for its electrochemical properties. According to Sameenoi et al [19], PDMS can be used as a sealing agent between the carbon composite electrode and a microfluidic system made in the same polymer, thanks to its physico-chemical properties (covalent bonding by plasma treatment, elasticity etc). Moreover, the electrodes made of carbon and PDMS show low capacitive current, which permits to reach lower limit of detection (LOD). The authors described a process in which they integrated a carbon-based paste into a micromolded microchannel in order to obtain a well-defined microband of 250 µm width for electrochemical detection of organic compounds (dopamine, with a LOD of 16.8 µM), in a microfluidic channel, thus showing the interest of carbon-based composite as material for electrochemical detection. Also, Deman et al. developed carbon/PDMS composites (C/PDMS) as materials to generate an electric field for the manipulation of particles and cells in microchip with similar fabrication pathways [20], showing the possible use of this kind of material in sealed PDMS microchip [21]. Nonetheless, the plasma treatment required to seal the electrode within the microchannel can be harmful, leading to an increase of the capacitive current and a decrease of the signal to noise ratio, thus altering the performance of the electrode for analytical applications. In this context, there is still a great need for a simple and gentle sealing process combined to an electrode regeneration/cleaning strategy since some passivation of the detection electrodes may occur over time .

All the above mentioned studies are related to the preparation and easy use of the microelectrodes within a monochannel at microscale but none of them was dedicated to the coupling of the electrochemical detection with a simultaneous electrophoretic separation. In this work, we propose a new homemade detection system that includes a composite working microband electrode made of C/PDMS (30 µm width) and either two other bands of C/PDMS (in

a 3-electrodes setup) as integrated reference and counter-electrodes, or a silver silver-chloride (Ag/AgCl) wire as pseudo-reference electrode (pseudo-RE) in a 2-electrodes setup. An easy and innovative integration strategy was also developed in a reopenable NOA-based microfluidic channel, allowing multiple repositioning of the microband electrode for robust analysis in reusable system. The coupling of this electrochemical detection with microchip electrophoresis was also demonstrated and optimized using $Ru(NH_3)_6^{3+}$, a model molecule

2. Experimental

2.1. Reagents

All reagents were of analytical grade: graphite powder noted as C (2-15 µm microcrystal grade 99.9995%, Alfa Aesar, Germany), PDMS RTV 615 kit (Momentiv, France), PDMS Sylgard 184 kit (Dow Corning, Germany), SU8 2075 (Microchem, USA), hexaamine ruthenium(III) chloride (noted as $Ru(NH_3)_6^{3+}$, 98%, Sigma Aldrich), ferrocene methanol (noted as FcMeOH, 97%, Sigma Aldrich), sodium phosphate dibasic (99%, Sigma Aldrich), sodium phosphate monobasic (99%, Sigma Aldrich), hydrochloric acid (HCl, 37%, Acros Organics), sodium chloride (NaCl, Bio-ultra ≥ 99.5 %, Sigma), potassium chloride (KCl, ≥ 99.5 %, Fluka) and ultrapure water (Purelab Flex System, Veolia, France) for preparation of aqueous solutions.

2.2. Micro-electrode fabrication

The C/PDMS electrodes were fabricated according to the method described in Figure 1: first, a SU8 mold was prepared by spin-coating a few milliliter of SU8 2075 on a silicon wafer (4″, Prolog Semicor Ltd, Ukraine), previously dried on a heated plate at 200°C for 15 min. The spread was performed for 15 s at 500 rpm and 30 s at 2000 rpm to obtain a theoretical thickness of 110 µm [22]. The wafer was then heated at 65°C for 10 min and 95°C for 20 min. A plastic mask containing the channel design (both 3-electrode and 2-electrode setup, described in Figure 2-a/b) was laid on the wafer prior to UV exposure (100% power for 11s UV-KUB 2 Kloé, France). The mask was obtained designing it on Clewin5 software and by printing it with a photoplotter Filmstar (Bernier Electronik, France) and Kimolek paper (Bernier Electronik, France). The wafer was then heated at 65°C for 5 min and 95°C for 10 min prior to the developing step which consists in immersing the wafer into propylene glycol monomethyl ether acetate (≥ 99.5%, Sigma-Aldrich) at 100 rpm for 15 min. The positive pattern was then revealed, according to the design of the mask. Sylgard PDMS was prepared by mixing the elastomer and the curing agent (from the kit) at a

ratio 10:1 prior to degassing. The mix was then poured on the silicon wafer containing the SU8 pattern, heated at 70°C for 1 h and unmolded to obtain the negative pattern in the PDMS substrate. The wafer can be reused to make multiple PDMS replica. A mix of PDMS and graphite powder was prepared as a conductive paste for microelectrode fabrication. The PDMS was made of a mix of RTV 615 elastomer and an associated curing agent (from the kit) at a ratio 10:1. The mix was made prior to the incorporation of graphite powder to avoid pre-reticulation that occurs even at ambient temperature. The paste was made in a plastic flask by properly mixing both components by hand with a spatula until complete integration of graphite powder and homogeneous paste, as already mentioned in the literature [20]. Other technics can be employed to mix both components, such as the use of a miller [18] or dispersion of components in toluene for easier mixing [16]. Then, the C/PDMS paste was spread with a spatula on the surface of the PDMS mold in order to fill the molded microchannel. The excess of paste was removed by carefully polishing the surface with paper and carbide paper (Presi, France). The electrode was then heated at 70°C for 3 h prior to use, to insure the complete reticulation of the mix.

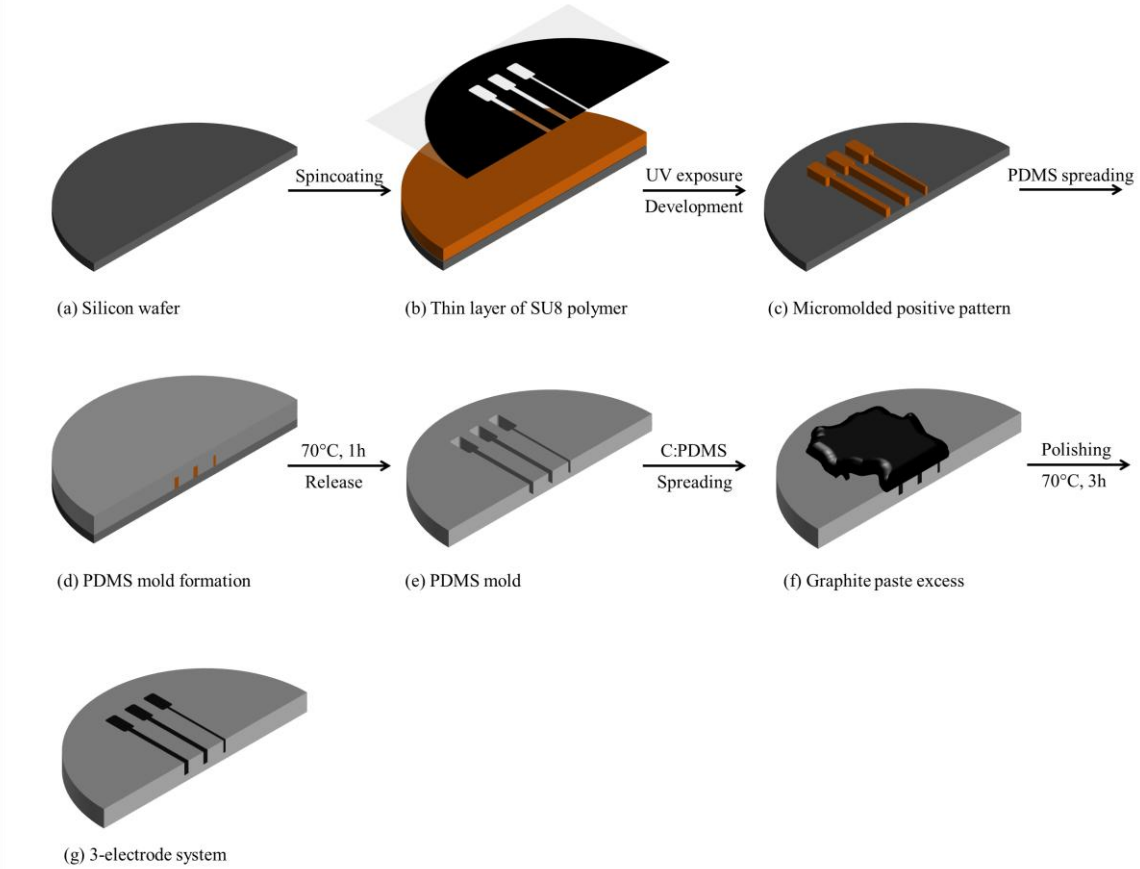

Figure 1 – Fabrication process of the 3-electrodes setup made of C/PDMS mix. The fabrication process of 2-electrodes system is similar, except the use of another mask that contains only 1 band.

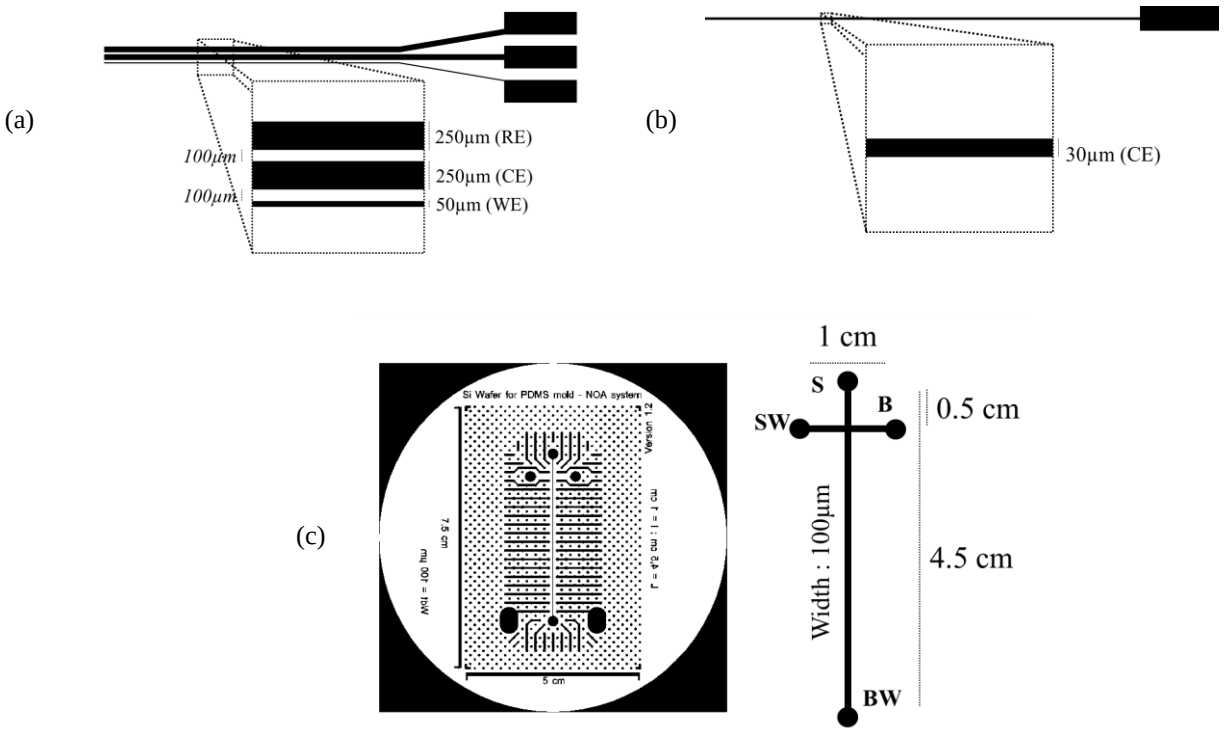

Figure 2 – Scheme of the (a) 3-electrodes setup, (b) 2 -electrodes setup and (c) mask for the fabrication of the microchip.

2.3. Microchip fabrication

The microchips were fabricated on glass slides previously pierced to create the wells for electrophoresis purpose with a LASER cutter (GCC Laser Pro-CO2 Laser Machine). The wells have to be perfectly aligned against the drawing of the mask to avoid any perturbations when using the setup for electrophoretic procedure. Briefly, a PDMS counter-mold (made by the methodology described above) containing the positive design (an illustration of the microchip mask used for the photolithographic process is shown in Figure 2-c) is degassed in a dessicator for 15 min and then is pressed on the glass slide previously covered with liquid Norland Optical Adhesive 81® (NOA81®, Epotecny, France). The NOA81 excess in the holes is removed with paper towels before exposition to 365 nm UV

light for 1 min (UV Biolink BLX, Vilber Lourmat, France) in order to complete the NOA81 reticulation. The PDMS counter-mold is then removed, leading to an open-microchannel molded in NOA81. Pipet tips (2-200 µL, Fischer Scientific, France) were cut and used as wells, fixed on top of glass holes with few amounts of NOA81 reticulated according to the same procedure. Two kind of chips were used for characterization and analysis respectively: the first one consists in a single channel of 3.5 cm length, 150 µm width and 40 µm height. The second one consists of a simple cross-shape section, with a separation channel of 100 µm width and 4 cm length, and the other channel of 100 µm width and 0.5 cm length (Figure 2-c). The wells are circles of 3 mm diameter. The additional channels and pillars are used for the fabrication, to remove bubbles and insure the horizontality of the setup when the PDMS counter-mold is pressed against the glass slide. This is required since the microchannel is sealed with the electrode PDMS support.

2.4. Scanning electron microscopy imaging

C/PDMS electrodes were characterized by Scanning electron microscopy (SEM). SEM images were acquired with SEM-FEG LEO 1530 (Zeiss) equipped with a PGT microanalyser with a Ge detector, after vaporization of a gold layer (about 5 nm) on the samples.

2.5. Electrochemical measurements

Electrochemical characterizations of C/PDMS electrodes were performed by cyclic voltammetry (CV) with a Model 263A Potentiostat/Galvanostat (Princeton Applied Research, USA) coupled with the Powersuite software for substrate electrodes, and an EA164 QuadStat with an E-corder 410 unit coupled with the EChem software for microelectrodes (eDAQ, Australia). The characterization of flat substrates was made with a 3-electrode setup (platinum wire as counter-electrode, CE, and silver-silver chloride wire as a pseudo-reference electrode). The characterization of the microband electrodes was made with a 3-electrode integrated setup (50 µm C/PDMS band as working electrode, and 250 µm C/PDMS band as CE and pseudo-RE, see Figure 2-a).

2.6. Chronoamperometric measurements coupled with electrophoresis microchip

Chronoamperometric measurements coupled with electrophoretic separation were performed with an isolated wireless potentiostat Model 9051 (Pinnacle, USA) on 30 µm C/PDMS electrodes placed in in-channel configuration (< 10 µm-off the exit) against the glass-NOA® cross microchip (Figure 2-c and Figure 3). High voltages applied for

the electric field were performed with an ER430 high voltage sequencer (eDAQ, Australia). Platinum wires (0.1 mm, 99.99%, Good Fellow) were used as electrodes for the application of the separation voltage, immersed in the wells that contain the background electrolyte (BGE) and the sample. An Ag-AgCl wire was used as CE and pseudo-RE for chronoamperometric experiments. The injection parameters for $Ru(NH_3)_6^{3+}$ were as follow: BGE made of HCl 1 $mmol.L^{-1}$ and NaCl 50 $mmol.L^{-1}$. A gated injection was performed, with a loading step with separation voltage such as: S = Ground, SW = -300 V, B = Ground, BW = -500 V for 100 s. The injection occurs for 2 s with: S = Ground, SW = -150 V, B = Float, SW = -1000 V. The separation was the same as the loading step, for higher analysis time. The detector was set at +0.1 V/Ag-AgCl. The studied solutions consist of $Ru(NH_3)_6^{3+}$ (from 250 to 10 $\mu mol.L^{-1}$) in the BGE. A washing with the BGE was performed between each measurement, by simply flowing it with a syringe. The measure of the electroosmotic flow (eof) was performed in the same conditions, except with a sample containing FcMeOH 0.2 mM in the same media and with a detection potential of +0.8 V/Ag-AgCl. It has to be noted that the eof was estimated to be less than 3.10^{-5} $cm^2.V^{-1}.s^{-1}$ since no signal was measured after more than 30 min of analysis.

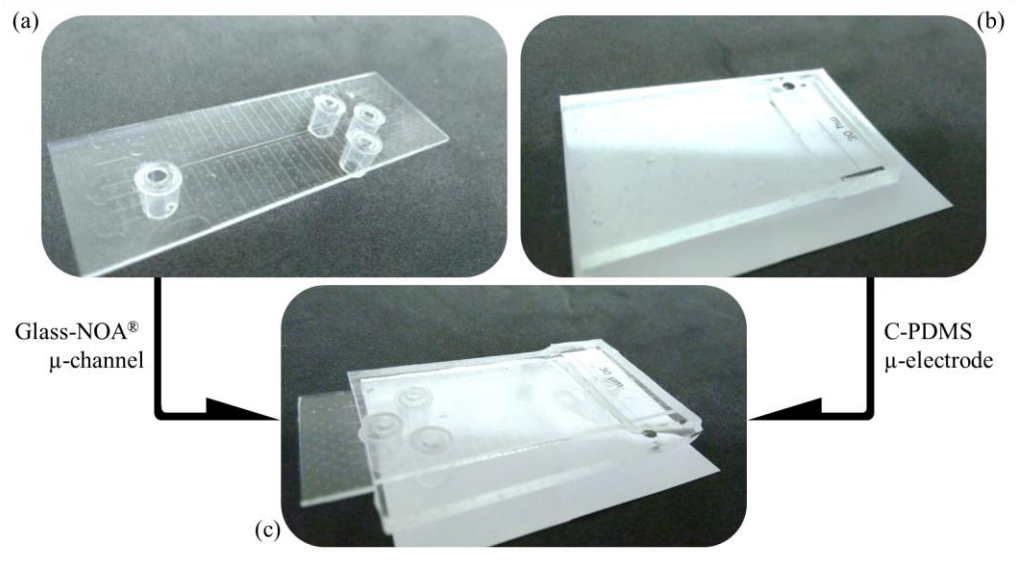

Figure 3 – Picture of (a) the Glass-NOA® microchannel, (b) the C-PDMS electrode and (c) the assembled device for electrophoretic analysis

3. Results & Discussion

3.1. Optimization of C/PDMS ratio for microelectrode preparation

The composite material conceived for microelectrode preparation is made of two compounds. The first is the conductive material, graphite powder with high purity (99,9995%) and a particle size inferior to 15 µm. The purity of the graphite powder is of importance since interfering electrochemical signal can occur if some electroactive species remain in the matrix (such as metals). The particle size was chosen for miniaturization of the microband electrode down to 30 µm, as discussed later. Preliminary experiments were carried out by preparing different mixtures of graphite powder and PDMS at different weight ratios to get optimized material in terms of ease of fabrication, ease of handling, electric conductivity and mechanical stability. To 1 g of PDMS mixture (composed of the monomer and a reticulating agent) prepared a few minutes before to avoid reticulation, the mixtures were obtained by addition of the corresponding amount of graphite powder and the obtained mixture was immediately mixed by hand with a spatula. Different C/PDMS mixtures were studied with w/w% ratios of 4/8, 5/8, 6/8, 7/8 and 8/8. Lower ratios could not be achieved since the graphite particles were too dispersed in the matrix after reticulation or gave a crumbly paste after a long mixing time respectively. The mixtures 4/8 and 5/8 gave a relatively viscous paste, easy to mix and spread on a glass slide. For ratios larger than 8/8, the amount of graphite powder was too high to be perfectly incorporated to the PDMS matrix, hindering their further use.. The fabrication process is reported in Figure 4. In order to obtain flat surfaces for characterization, the pastes were spread onto microscope glass slides with a spatula before curing (step 1). The spreading is less and less easy while the percentage of graphite increases in the paste, but is still possible if the paste is correctly mixed. The reticulation of the paste for the solidification of the electrode is insured by a heating step. According to the supplier, PDMS, is usually activated and reticulated during 1 h at 70°C. The heating step for the reticulation of the composite has been optimized for 3 h instead of 1 h, as lower curing time led to disintegration of the composites and/or sticking to the glass slide (step 3). The presence of graphite powder seems to affect the kinetics of the PDMS reticulation, especially when the C/PDMS ratio is the highest (7/8 and 8/8). The composites with those latter ratios were so fragile that the addition of PDMS on top of the substrate was required in order to ensure the physical integrity of the electrode (step 2) and to disband them from the glass slide (step 4).

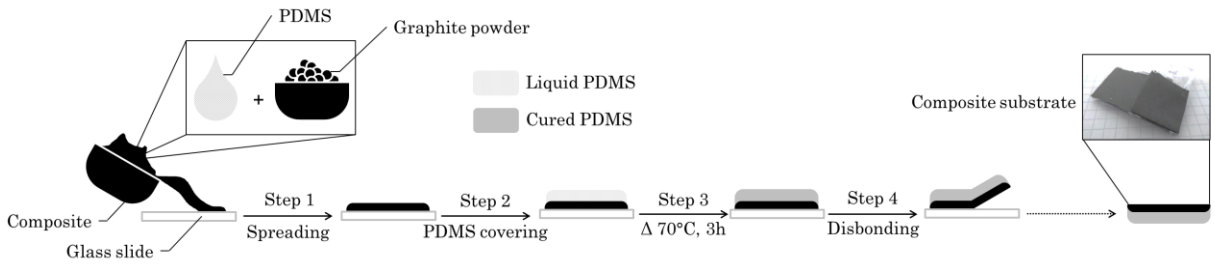

Figure 4 – Fabrication process of the composite substrate made of graphite powder and PDMS

The electrochemical properties of the different C/PDMS electrodes were studied by using $Ru(NH_3)_6^{3+}$ and FcMeOH as redox probes. A preliminary study was first conducted by delineating a disk-shaped electrode by using a PDMS stamp, in which a 6 mm diameter hole has been pierced with a puncher. For each substrate, the adhesion was good and no leakage was to mention. Solutions were poured in the well, while RE and CE were immersed into the well (Figure 5-a).

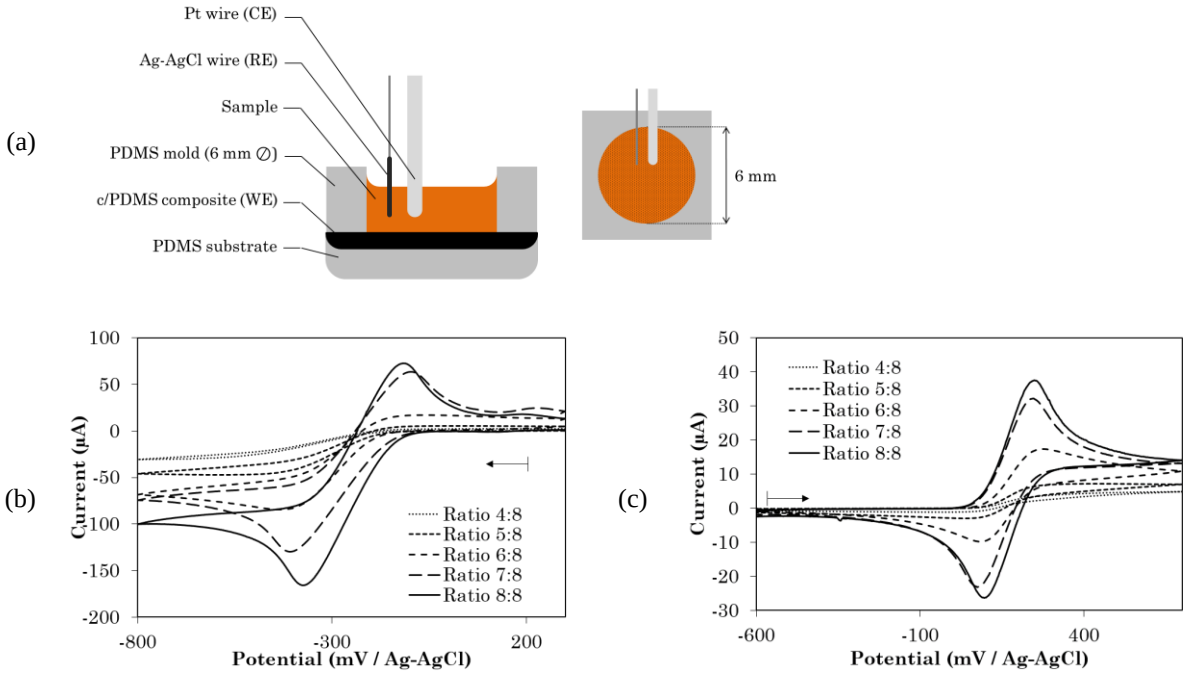

Figure 5 – Scheme of the electrolytic cell with C/PDMS as working electrode WE (a). Cyclic voltammetry on C/PDMS electrodes of (b) 5 mmol.L^{-1} $Ru(NH_3)_6^{3+}$ and (c) 1mmol.L^{-1} FcMeOH. Electrolyte : 50mmol/L^{-1} phosphate buffer (pH 6.7). WE = C/PDMS 8/8 circular (diameter 6 mm delimited by a PDMS stamp), pseudo-RE = Ag-AgCl wire, CE = Pt wire. Scan rate 25 mV.s^{-1}.

Cyclic voltammograms of the electrodes were performed for each ratio to evaluate its influence on the electrochemical behavior of the composite material. For C/PDMS ratios of 4/8 and 5/8, the cyclic voltammogramms show a reduction wave-shaped signal related to the reduction of Ru(+III) to Ru(+II) (Figure 5-a) and the oxidation of

Fe(+II) to Fe(+III) (Figure 5-b). For larger C/PDMS ratios, the cyclic voltammograms exhibit the classical peak-shaped signals obtained at millimetric electrodes. The difference in shape of the voltammograms for both probes (wave versus peak) may be attributed to the fact that, for lower graphite content in the composite, the surface forms a network of micrometric conductive parts, which can be assimilated to a network of separated microelectrodes with a radial diffusion and no overlapping of the diffusion layer. In this case, a wave signal is obtained, as for an ensemble of simultaneously addressed ultramicroelectrodes (UMEs). As the C/PDMS ratio increases, the shape of the cyclic voltammogramms gradually moves from a wave-shaped signal to a peak-shaped one. For C/PDMS ratios of 8/8, the voltammogramms exhibit anodic and cathodic peaks for both redox probes, with a quasi-reversible behavior, characterized by peak-to-peak separation of 229±26 mV for $Ru(NH_3)_6^{3+}$and 168±21mV for FcMeOH. The highest peak intensities are obtained for the larger ration C/PDMS 8/8, with -163±12 µA and 35±4 µA for $Ru(NH_3)_6^{3+}$ and FcMeOH, respectively. The difference in peak current intensity between both probes is essentially due to their difference in concentrations ($Ru(NH_3)_6^{3+}$ being studied at 5 mmol L^{-1} and FcMeOH at 1 mmol L^{-1}, both probes having close diffusion coefficient values (5.5 10^{-5} cm^2/s and 7.8 10^{-5} cm^2/s, respectively) [23–25]. These results are in good agreement with the fact that the graphite powder acts as the unique conductive part of the composite. The real electrode surface was estimated to 79 to 85 % of the theoretical geometric area, by conducting chronoamperometric measurements in $Ru(NH_3)_6^{3+}$ and FcMeOH solutions and then exploiting them using the Cottrell equation at short time scale in solutions (see Supporting information).

C/PDMS ratio 8/8 was chosen for the miniaturization of the electrode in a microband electrode format since mechanical properties of the paste before reticulation constrain the fabrication methodology (too much graphite leads to crumbly paste, unuable).

3.2.Microelectrode format and characterization

A microband electrode was fabricated with two width values of 50 µm or 30 µm. They were characterized by SEM and electrochemistry (CV experiment) using a 3-electrodes setup integrated in a microsystem (see below).

3.2.1. SEM characterization

The microband electrodes (50 and 30 µm width) were first characterized by SEM, as shown on Figure 6. A band of C/PDMS 8/8 of regular width of around 50 µm and 35 µm are observed respectively, in good agreement with the expected size and shape from the prepared molds. For both microband electrode widths, the edges are straight and the surface of the electrode is quite uniform with almost no imperfections. The absence of graphite outside of the

channel indicates that the polishing step, aiming at removing the excess of composite, is appropriate for the microfabrication and does not affect the bonding between PDMS matrix and the NOA® channels. The homogeneity of the surface is also an indicator of the proper mixing of the paste and of the efficiency of the polishing. Moreover, it can be seen on the SEM pictures that the microparticles of graphite look like a superposition of leaflets. The EDS analysis of both C/PDMS composite and PDMS substrate (data not shown) shows a larger concentration of C atom in the microelectrode area compared to the polymer alone, which is in good agreement with its formulation, mainly composed of graphite powder.

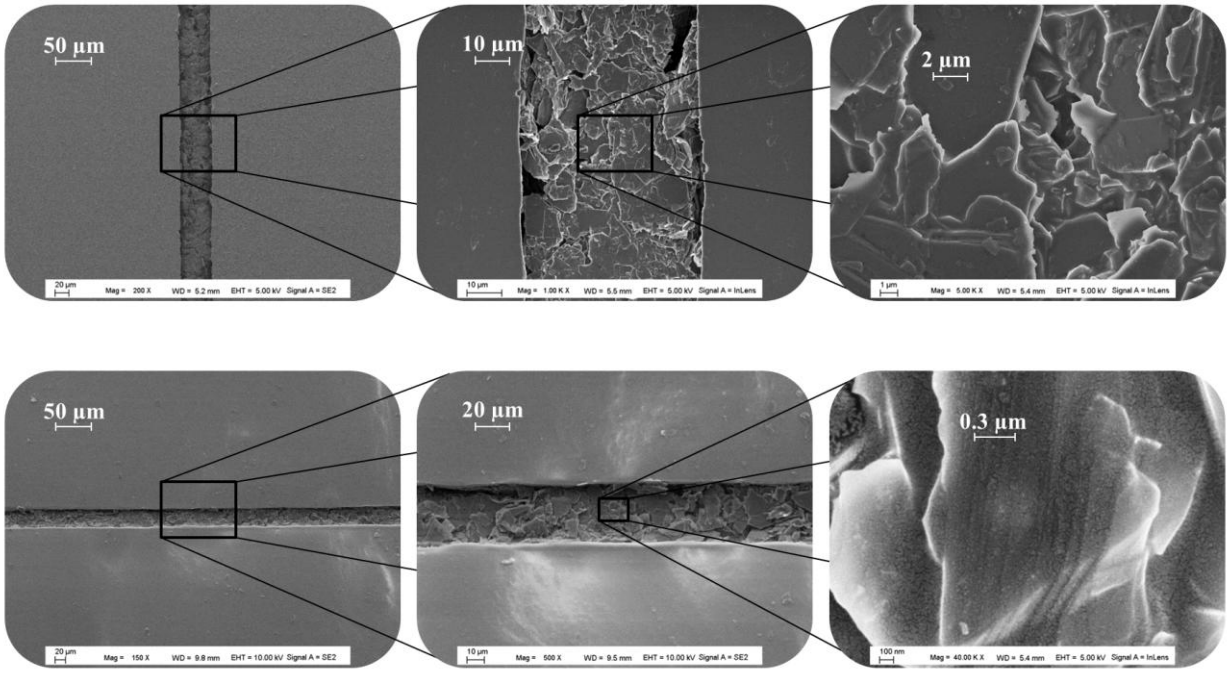

Figure 6 –SEM images of C/PDMS electrode (50 µm (top) and 30 µm (bottom) width band)

3.2.2. Electrochemical characterization

The electrochemical characterization of the microband electrode has been performed using $Ru(NH_3)_6^{3+}$ and FcMeOH as redox probes. A 3-electrodes setup has been integrated into microfluidic device, by positioning the microband electrodes perpendicularly to a glass-NOA® microchannel of 150 µm width and 40 µm height. The dimensions of this setup were inspired by the commercially available Micrux® microchip. The 50 µm width microband was used as the working electrode. The second band (250 µm width) was used as a CE and the last one (250 µm width) was used as a pseudo-RE. All the electrodes were positioned inside the microchannel to clearly define the electroactive surface. The channel was filled with the redox probe solution and the CV acquired, as illustrated on Figure 7.

Between each acquisition, the channel was rinsed with the buffer and the solution renewed to insure the repeatability of the measurements. Moreover, the chip was opened and the electrodes repositioned three times in order to place the microchannel opposite to a new spot of the strip electrode, to avoid any pollution that could remain after analysis and to prove the relevance and robustness of such a dismountable microchip.

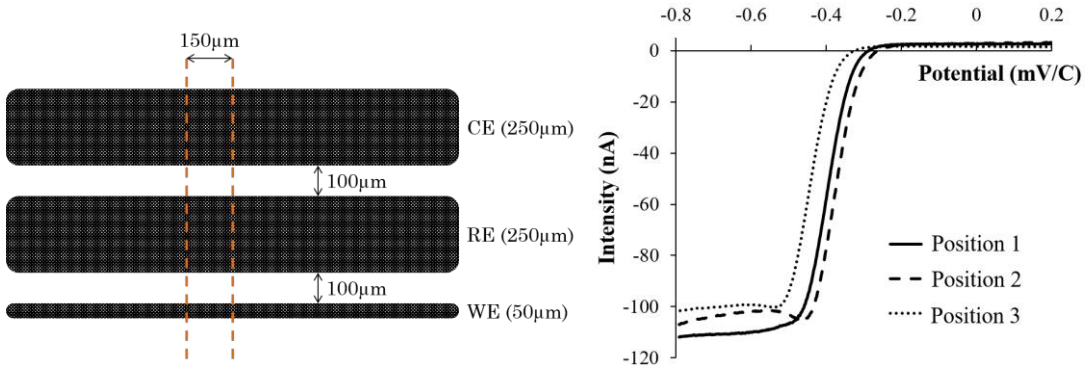

Figure 7 – Design of the 3-electrodes C/PDMS set up(left). Linear voltammetry of 5 mmol.L^{-1} Ru(NH$_3$)$_6^{3+}$ on this design integrated in a glass-NOA® microchannel (right). Electrolyte : 50 mmol.L^{-1} phosphate buffer (pH 6.7). WE : C/PDMS 50x150 µm, pseudo-RE : C/PDMS 250x150 µm, CE: C/PDMS 250x150 µm. Scan rate 25 mV.s^{-1}. Three measurements were performed on each working electrodes.

The CV of Ru(NH$_3$)$_6^{3+}$ shows a signal characteristic of that of an UME, with an half-wave reduction potential of -404 ± 25 mV and wave intensity of -15,0 ± 2.4 µA/mm^2 . That FcMeOH shows similar features with an half-wave oxidation potential of +322 ± 40 mV and wave +1,5 ± 0.3 µA/mm^2 (data not shown)[1].

The experimental current density is higher on the microelectrode format than on the millimetric one in both cases (-15 vs -5.9 and 1.5 vs 1.3 µA/mm^2 for Ru(NH$_3$)$_6^{3+}$ and FcMeOH respectively), as expected and in favor to the miniaturization of the composite electrode. The use of the 3-electrodes setup can be considered for electrochemical detection in microsystem since the variability of the different tested electrodes was low (< 20%, N = 9), for chronoamperometry measurement for example.

The influence of the pseudo-RE nature (C/PDMS versus siver/silver chloride) on the electrochemical behavior was evaluated. The current density generated using a Ag/AgCl wire as pseudo-RE and positioned inside the well of the

[1] The estimation of the theoretical current generated on a microelectrode band during CV experiment can be calculated using eq.1 [26,27]:

$$I_{th,max} = n.F.C_i.L.D_i.\left(0.439p + 0.713p^{0.108} + \frac{0.614p}{1+10.9p^2}\right) \quad \text{eq. 1}$$

With $= \sqrt{\frac{n.F.v.w^2}{R.T.D_i}}$, w width of the electrode (50 µm) and L length of the electrode (150 µm).

For this configuration, theoretical current density values of -9.1 µA/mm^2 and 2.4 µA/mm^2 were calculated for Ru(NH$_3$)$_6^{3+}$ and FcMeOH respectively. These values correspond, according to the experiment, to an active surface of 164% and 65%, which is clearly variable compare to what is expected theoretically (and compare to what was obtained on substrate format). This can be attributed either to different migration mechanism due to shape and roughness of the electrode, but also to the fact that the equation is initially adapted to planar microelectrode band, which is not the case here.

microchip was proved to lead to the same value for $Ru(NH_3)_6^{3+/2+}$, but with a half-wave of -347±15 mV, slightly different from the one on the integrated C/PDMS pseudo-RE. The standard potential value for $Ru(NH_3)_6^{3+/2+}$ is +0.10 V/NHE, so that the potential of the pseudo-RE C/PDMS can be estimated to +0.50 V/NHE in the phosphate buffer.

The successful fabrication of miniaturized band electrodes was performed with widths as low as 30 µm, which is smaller than what was previously described in the literature (250 µm [19] and 100 µm width [11]). Moreover, the cost for the fabrication of ten microelectrodes on PDMS substrate can be estimated to 1.04 € (2 g PDMS + 100 mg graphite powder), which is quite low compared to other systems [11].

3.3. Coupling of the amperometric detector with electrophoresis in a microdevice: Application to the quantitation of $Ru(NH_3)_6^{3+}$

The coupling of electrochemical detection with microchip electrophoresis requires some precautions, due to interferences that can occur between the electric fields generated for both methods. Indeed, the electrophoretic migration of ions under an electric field requires the application of a difference of potential in the microchannel of the microfluidic system. This electric field (typically of more than 100 $V.cm^{-1}$) can have a strong impact on any electrochemical detector placed inside the separation channel, since it brings some noise and interference with the electric field used for the electrochemical detection [4]. This effect was evaluated by conducting cyclic voltammetry of $Ru(NH_3)_6^{3+}$ placed in a microchannel, with or without the application of a separation voltage for electrophoresis and using a 50 µm C/PDMS WE. Two configurations were tested, with the electrode system at the end of the channel (i.e.in the outlet reservoir, “end-channel” configuration) or withing the separation channel (“in-channel” configuration).

3.3.1. End-channel detection mode

The 3-electrodes setup was placed into a single microchannel, in the end-channel configuration as illustrated on Figure 8, and CV were performed under a separation voltage within the microchannel of different values. The influence of the nature of the pseudo-RE (either C/PDMS or Ag/AgCl) was also studied .

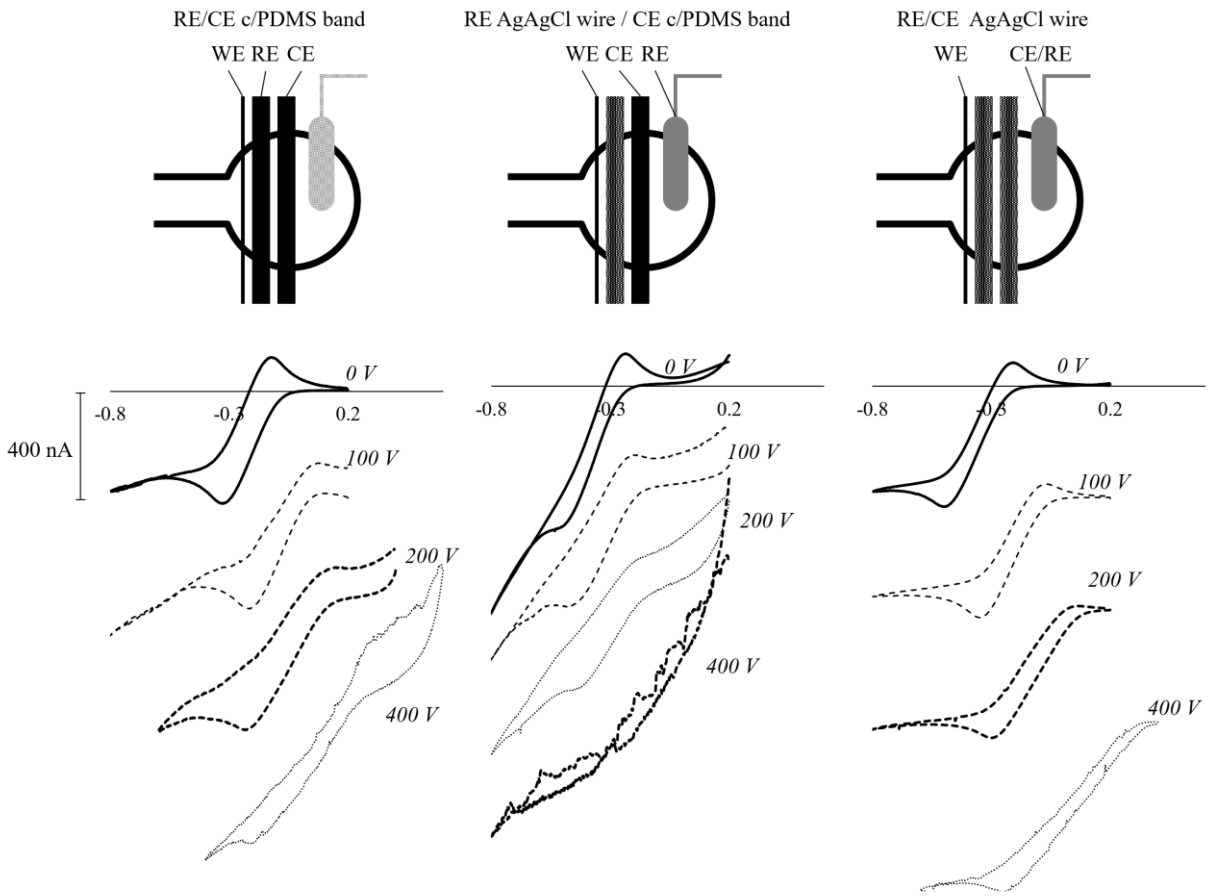

Figure 8 – Influence of RE and CE natures on the cyclic voltammograms of 5mM $Ru(NH_3)_6^{3+}$ in the end-channel configuration. Separation microchannel filled with $Ru(NH_3)_6^{3+}$. Electrophoretic separation voltage : 0 to +400 V. Scan rate : 25 mV/s.

For all RE and CE natures,, the potential for the reduction of the probe is shifted to more positive values and the noise increases when separation voltage increases, , as reported in the literature [5]. The shift in potential can be explained by the interaction between the electric field for the separation and the one for the detection, while the noise increase can be attributed to higher Joule effect under higher electric field value (100 $V.cm^{-1}$). Secondly, the use of a pseudo-RE made of an Ag/AgCl wire leads to lower shift of the reduction potential (from -0.37 V with no separation voltage to -0.29 V at +200 V) in comparison to the use of C/PDMS pseudo-RE band (from -0.23 V with no separation voltage to -0.04 V at +200 V). Thirdly, the use of an external Ag/AgCl wire concomitantly as pseudo-RE and CE leads to a better stability of the signals and a lower noise, even for the highest electric field (+400 V) C/PDMS microband is therefore not recommended when integrated as a pseudo-RE in an electrophoretic microdevice with electrochemical detection. On the contrary, Ag/AgCl wire provides a higher stability of the reduction potential value when applying an electric field for electrophoretic separation. Moreover, the use of short-

circuited Ag/AgCl pseudo-RE/CE (in a 2-electrodes configuration) seems to give an even better signal than with a 3-electrodes setup. Finally, the CV do not show the behavior of a microelectrode, which can be explained by the fact that the microband electrode (WE) is placed in end-channel configuration, thus leading to a larger electrode surface.

3.3.2. In-channel detection mode

The end-channel configuration used previously suffers from another drawback: since the WE is placed outside the microchannel (i.e. in the outlet reservoir), the sample undergoes a dilution in this reservoir which leads to a loss in analytical performances [5]. To overcome this drawback, the in-channel configuration was tested, where the WE is positioned within the separation microchannel to avoid the sample dilution. For this configuration, the use of a classical potentiostat is to be avoided since the separation voltage for the electrophoretic separation can damage the device if not grounded, so that a wireless potentiostat has to be used for the chronoamperometric detection. This is only compatible with a 2-electrodes setup where the pseudo-RE and the CE are short-circuited [28]. Chronoamperometric measurements were performed (Figure 9) to evidence any influence of the electric field on a 2-electrodes setup in an in-channel configuration (cross-shape system). The set up consisted in a C/PDMS microband electrode of 30 µm width placed just before the end of the separation channel and a pseudo-RE/CE made of an Ag/AgCl wire immersed in the nearest well. The microband width was selected at 30 µm since it gave less noise than larger electrodes, thus leading to lower LOD.

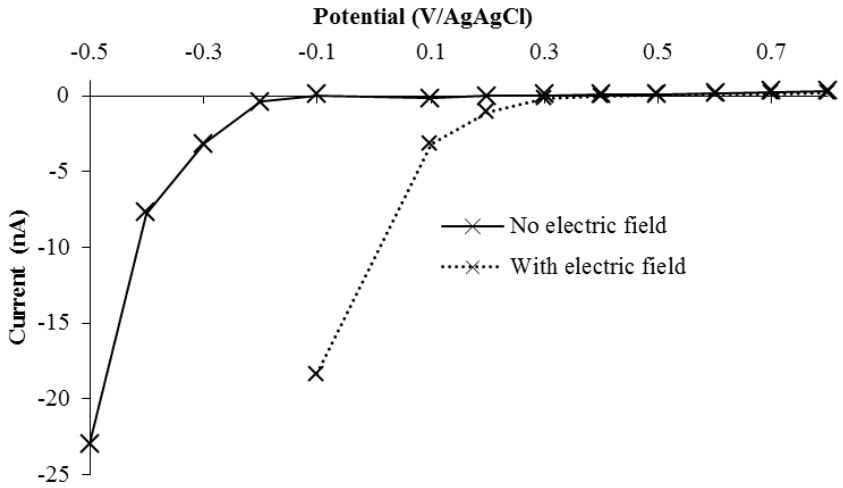

Figure 9 – Influence of a separation electric field on the chronoamperometric current of 250 µmol.L^{-1} $Ru(NH_3)_6^{3+}$ in a in-channel configuration . Background electrolyte: 1 mmol.L^{-1} HCl and 50 mmol.L^{-1} NaCl. Separation voltage : S = Ground, SW = -300 V, B = Ground, BW = -500 . Current measured 30s after application of the corresponding potential. WE : 30 µm width C/PDMS,, CE/RE = AgAgCl wire immersed in well BW. This representation corresponds to the substraction of blank (BGE alone)

In the absence of the separation voltage, $Ru(NH_3)_6^{3+}$ could not be reduced for potential values superior to -0.1V/AgAgCl. When applying the separation voltage, a reduction signal of $Ru(NH_3)_6^{3+}$ could be obtained for a potential up to +0.3 V/AgAgCl. Therefore, the 2-electrodes set-up in a in-channel configuration is efficient for the detection of the redox probe at a detection potential inferior to +0.1V/AgAgCl .

3.3.3. Analytical performances for the electrophoretic separation and detection of $Ru(NH_3)_6^{3+}$

Finally, the 2-electrodes setup was employed for the separation and in-channel chronoamperometric detection of $Ru(NH_3)_6^{3+}$ in the microfluidic device. The BGE was composed of 1 $mmol.^{L-1}$ HCl and 50 $mmol.L^{-1}$ NaCl since this media will be used for further applications in the same device. For this purpose a "gated" injection mode (Figure 10 c) was developed, followed by an electrophoretic separation (with a gated injection mode) and a chronoamperometric detection at +0.1 V/Ag/AgCl. The electrophoregram (a) and the calibration curve for the quantitation (b) from 10 to 250 $\mu mol.L^{-1}$ are presented in Figure 10,

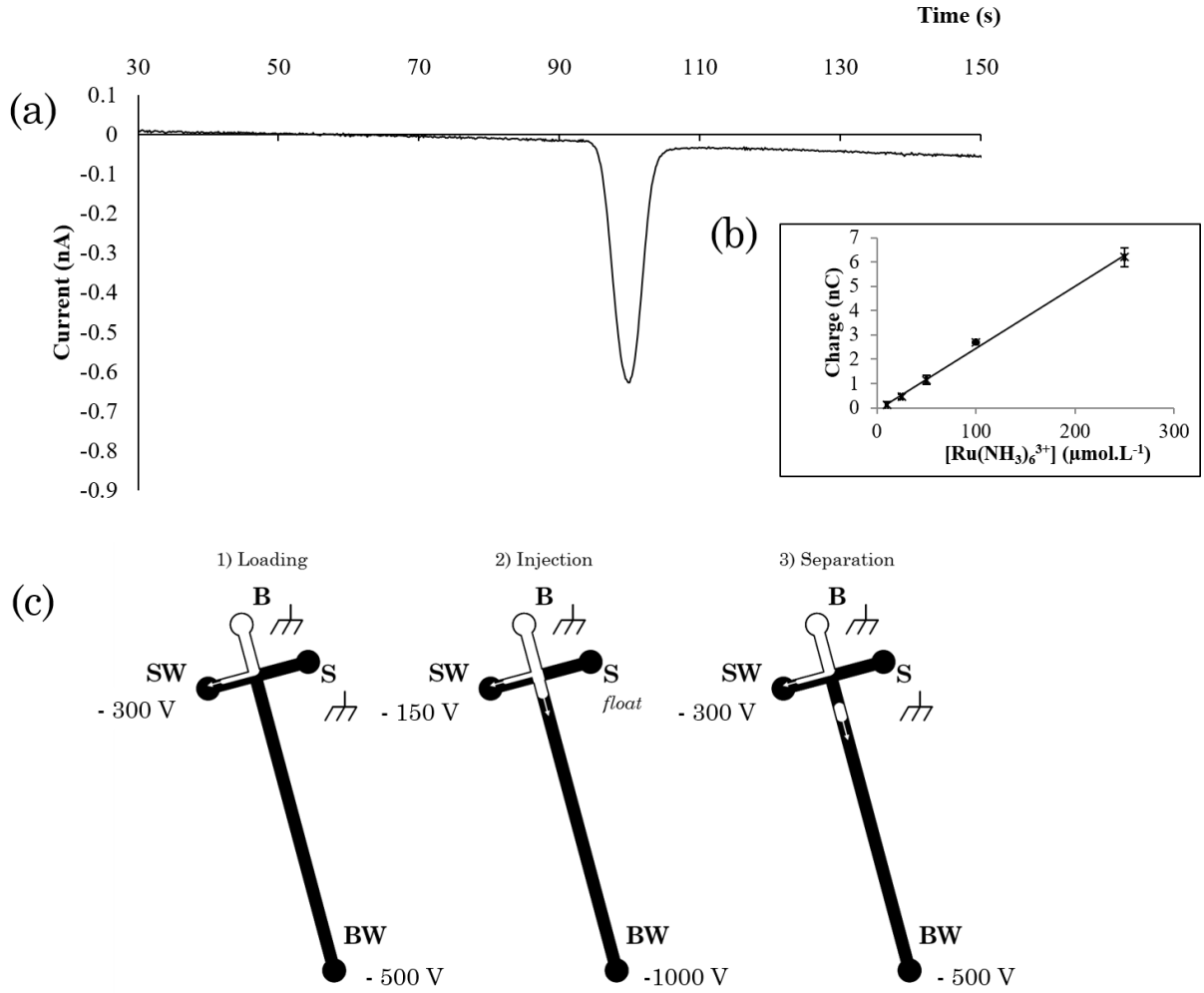

Figure 10 – (a) Electropherogram of 100 µmol.L^{-1} $Ru(NH_3)_6^{3+}$ with in-channel chronoamperometric detection. Conditions for separation described in materials and methods section. (b) Calibration curve for $Ru(NH_3)_6^{3+}$ (Charge = f([$Ru(NH_3)_6^{3+}$], from 250 to 10 µmol.L^{-1}). (c) Scheme of the electrokinetic sequence and conditions for sample loading, injection and separation.

Since the electroosmotic flow is negligible (data not shown), the electrophoretic mobility of $Ru(NH_3)_6^{3+}$ was directly estimated from its migration time, equal to 35.7 ± 0.7 10^{-5} $cm^2.V^{-1}.s^{-1}$ (average value of 15 acquisitions). Reproducibility was assessed by employing two other zones of the same electrode after opening the chip and shifting the channel position, and led to comparable signal intensity under the same conditions (variability < 5%). The use of the dismountable system is proved to be effective, permitting to use the same microelectrode several times on different spots of the band, which increases the lifetime of the detection part.

A linear regression was obtained between the signal area and the analyte concentration ranging from 10 to 250 µmol.L^{-1}. The limit of detection (S/N = 3) and the limit of quantitation (S/N =10) were 3.4 and 11.3 µmol.L^{-1}, respectively. Therefore,C/PDMS based microelectrodes were proved suitable for electrophoretic separation coupled to chronoamperometric detection.

4. Conclusion

A new microfluidic device has been developed, consisting in an openable sandwich microdevice system made of two parts (1) a microchannel micromolded in NOA® on a glass slide, and (2) a PDMS matrix on which is integrated a screen-printed C/PDMS band microelectrode of 30 µm width. This electrode has been characterized by electrochemistry, providing good reproducibility. The SEM images indicate a homogeneous electrode surface and well defined electrode bands. Its use for chronoamperometry coupled with electrophoretic separation has been demonstrated with the quantitation of $Ru(NH_3)_6^{3+}$ in acidic media, by coupling a high separation voltage with a wireless potentiostat for amperometric detection. This analytical method led to a limit of detection of 3.4 µmol.L^{-1} for $Ru(NH_3)_6^{3+}$, with an analysis time inferior to 2 minutes. This openable system allows to easily wash the microchannel, but also renew the electrode surface by simply repositionning the microband, showing a variability of less than 5%, and increasing its lifetime.

5. Acknowledgements

This work was supported by the French Environment and Energy Management Agency (ADEME) and the Chaire "Mines Urbaines" from ParisTech foundation, supported by Eco-systèmes. This work has received support of "Institut Pierre-Gilles de Gennes" (Laboratoire d'excellence: ANR-10-LABX-31, "Investissements d'avenir": ANR-10-IDEX-0001-02 PSL and Equipement d'excellence: ANR-10-EQPX-34). P. Vermaut from Institut de Recherche de Chimie Paris, CNRS 8247, Team Métallurgie structurale, Chimie ParisTech, is gratefully acknowledged for SEM imagery.

6. References

[1] H. Gai, Y. Li, E.S. Yeung, Optical Detection Systems on Microfluidic Chips, in: Microfluidics, Springer, Berlin, Heidelberg, 2011: pp. 171–201. doi:10.1007/128_2011_144.

[2] X. Feng, B.-F. Liu, J. Li, X. Liu, Advances in coupling microfluidic chips to mass spectrometry, Mass Spectrom. Rev. 34 (2015) 535–557. doi:10.1002/mas.21417.

[3] L. Nyholm, Electrochemical techniques for lab-on-a-chip applications, Analyst. 130 (2005) 599–605. doi:10.1039/B415004J.

[4] F.-M. Matysik, Advances in amperometric and conductometric detection in capillary and chip-based electrophoresis, Microchim. Acta. 160 (2008) 1–14. doi:10.1007/s00604-007-0802-3.

[5] W.R. Vandaveer, S.A. Pasas-Farmer, D.J. Fischer, C.N. Frankenfeld, S.M. Lunte, Recent developments in electrochemical detection for microchip capillary electrophoresis, ELECTROPHORESIS. 25 (2004) 3528–3549. doi:10.1002/elps.200406115.

[6] Microfluidic Chip Holder | MicruX, (n.d.). https://www.micruxfluidic.com/en/microfluidic-solutions/microfluidic-platforms-/microfluidic-chip-holder/ (accessed April 16, 2019).

[7] A.J. Gawron, R.S. Martin, S.M. Lunte, Fabrication and evaluation of a carbon-based dual-electrode detector for poly(dimethylsiloxane) electrophoresis chips, Electrophoresis. 22 (2001) 242–248. doi:10.1002/1522-2683(200101)22:2<242::AID-ELPS242>3.0.CO;2-W.

[8] M.L. Kovarik, M.W. Li, R.S. Martin, Integration of a carbon microelectrode with a microfabricated palladium decoupler for use in microchip capillary electrophoresis/electrochemistry, Electrophoresis. 26 (2005) 202–210. doi:10.1002/elps.200406188.

[9] R. Scott Martin, A. J. Gawron, B. A. Fogarty, F. B. Regan, E. Dempsey, S. M. Lunte, Carbon paste-based electrochemical detectors for microchip capillary electrophoresis/electrochemistry, Analyst. 126 (2001) 277–280. doi:10.1039/B009827M.

[10] M. Pumera, A. Merkoçi, S. Alegret, Microchip Capillary Electrophoresis-Electrochemistry with Rigid Graphite-Epoxy Composite Detector, Electroanalysis. 18 (2006) 207–210. doi:10.1002/elan.200503382.

[11] A. Regel, S. Lunte, Integration of a graphite/poly(methyl-methacrylate) composite electrode into a poly(methylmethacrylate) substrate for electrochemical detection in microchips, Electrophoresis. 34 (2013) 2101–2106. doi:10.1002/elps.201300055.

[12] A. Nag, N. Afasrimanesh, S. Feng, S.C. Mukhopadhyay, Strain induced graphite/PDMS sensors for biomedical applications, Sens. Actuators Phys. 271 (2018) 257–269. doi:10.1016/j.sna.2018.01.044.

[13] A. Nag, M.E.E. Alahi, S. Feng, S.C. Mukhopadhyay, IoT-based sensing system for phosphate detection using Graphite/PDMS sensors, Sens. Actuators Phys. 286 (2019) 43–50. doi:10.1016/j.sna.2018.12.020.

[14] L.O. Prasad, S.S. Pillai, S. Sambandan, Micro-Strain and Temperature Sensors for Space Applications with Graphite-PDMS Composite, in: 2019 IEEE Int. Conf. Flex. Printable Sens. Syst. FLEPS, 2019: pp. 1–3. doi:10.1109/FLEPS.2019.8792312.

[15] W.-P. Shih, L.-C. Tsao, C.-W. Lee, M.-Y. Cheng, C. Chang, Y.-J. Yang, K.-C. Fan, Flexible Temperature Sensor Array Based on a Graphite-Polydimethylsiloxane Composite, Sensors. 10 (2010) 3597–3610. doi:10.3390/s100403597.
[16] J.E.Q. Quinsaat, I. Burda, R. Krämer, D. Häfliger, F.A. Nüesch, M. Dascalu, D.M. Opris, Conductive silicone elastomers electrodes processable by screen printing, Sci. Rep. 9 (2019) 1–11. doi:10.1038/s41598-019-49939-8.
[17] M.A. Unger, H.P. Chou, T. Thorsen, A. Scherer, S.R. Quake, Monolithic microfabricated valves and pumps by multilayer soft lithography, Science. 288 (2000) 113–116.
[18] X.Z. Niu, S.L. Peng, L.Y. Liu, W.J. Wen, P. Sheng, Characterizing and Patterning of PDMS-Based Conducting Composites, Adv. Mater. 19 (2007) 2682–2686. doi:10.1002/adma.200602515.
[19] Y. Sameenoi, M.M. Mensack, K. Boonsong, R. Ewing, W. Dungchai, O. Chailapakul, D.M. Cropek, C.S. Henry, Poly(dimethylsiloxane) cross-linked carbon paste electrodes for microfluidic electrochemical sensing, Analyst. 136 (2011) 3177–3184. doi:10.1039/C1AN15335H.
[20] A.-L. Deman, M. Brun, M. Quatresous, J.-F. Chateaux, M. Frenea-Robin, N. Haddour, V. Semet, R. Ferrigno, Characterization of C-PDMS electrodes for electrokinetic applications in microfluidic systems, J. Micromechanics Microengineering. 21 (2011) 095013. doi:10.1088/0960-1317/21/9/095013.
[21] M. Brun, J.-F. Chateaux, A.-L. Deman, P. Pittet, R. Ferrigno, Nanocomposite Carbon-PDMS Material for Chip-Based Electrochemical Detection, Electroanalysis. 23 (2011) 321–324. doi:10.1002/elan.201000321.
[22] SU-8 2000 - MicroChem, (n.d.). http://microchem.com/Prod-SU82000.htm (accessed May 9, 2019).
[23] W. Miao, Z. Ding, A. Bard, Solution Viscosity Effects on the Heterogeneous Electron Transfer Kinetics of Ferrocenemethanol in Dimethyl Sulfoxide−Water Mixtures, J. Phys. Chem. B - J PHYS CHEM B. 106 (2002). doi:10.1021/jp013451u.
[24] J.E. Baur, R.M. Wightman, Diffusion coefficients determined with microelectrodes, J. Electroanal. Chem. Interfacial Electrochem. 305 (1991) 73–81. doi:10.1016/0022-0728(91)85203-2.
[25] A.J. Bard, L.R. Faulkner, Electrochemical Methods: Fundamentals and Applications, Wiley, 2000.
[26] K. Aoki, K. Tokuda, Linear sweep voltammetry at microband electrodes, J. Electroanal. Chem. Interfacial Electrochem. 237 (1987) 163–170. doi:10.1016/0022-0728(87)85229-4.
[27] S. Daniele, C. Bragato, From Macroelectrodes to Microelectrodes: Theory and Electrode Properties, in: L.M. Moretto, K. Kalcher (Eds.), Environ. Anal. Electrochem. Sens. Biosens. Fundam., Springer New York, New York, NY, 2014: pp. 373–401. doi:10.1007/978-1-4939-0676-5_15.
[28] Isolated wireless potentiostat, (n.d.). https://www.pinnaclet.com/pinnacle-handheld-isolated-potentiostat.html (accessed April 16, 2019).